Addressing the Ultra-Central Puzzle with Initial-State Nuclear Structures

Qi Wang(王琪), Long-Gang Pang(庞龙刚)*, and Xin-Nian Wang(王新年)*

Key Laboratory of Quark and Lepton Physics (MOE) and Institute of Particle Physics, Central China Normal University, Wuhan 430079, China

(Received 22 September 2025; accepted manuscript online 16 December 2025)

Hydrodynamic models fail to describe the near-equal v_3/v_2 ratio observed in ultra-central heavy-ion collisions, despite their success in other centrality classes. This failure can not be resolved by adjusting the shear viscous coefficient, as shear viscosity suppresses higher-order anisotropic flows more strongly, leading to an underestimation of v_3 when v_2 matches experimental data. To address this issue, we explore two initial-state modifications to resolve this puzzle: (1) impose a minimum distance between nucleons to simulate the homogenization effect arising from short-range nucleon–nucleon repulsion; and (2) introduce sub-nucleonic structures, specifically "hot spots" within protons, to provide a more refined description of initial-state fluctuations. Using TRENTo initial conditions and 3+1D viscous hydrodynamic model CLVisc, both approaches significantly lower geometric eccentricity, reduce required viscosity, and narrow the v_2-v_3 gap in ultra-central collisions. Our results implicate initial-state nuclear and sub-nucleon structures as critical factors in addressing this puzzle. Resolving it would advance nuclear structure studies and improve precision in extracting quark–gluon plasma (QGP) transport coefficients (e.g., shear viscosity), bridging microscopic nuclear features to macroscopic QGP properties.

DOI: 10.1088/0256-307X/43/2/020101 CSTR: 32039.14.0256-307X.43.2.020101

1. Introduction. The study of matter under extreme conditions of temperature and density represents one of the most vibrant frontiers in high-energy nuclear physics. Quark–gluon plasma (QGP), a deconfined state of quarks and gluons, is theorized to have filled the universe microseconds after the Big Bang. Through relativistic heavy-ion collision experiments conducted at facilities like the Relativistic Heavy Ion Collider (RHIC) and the Large Hadron Collider (LHC), this primordial state of matter is recreated momentarily in the laboratory, often metaphorically described as creating a "little bang".[1–4] The primary scientific objective of these endeavors is to probe the behavior of quantum chromodynamics—the theory of the strong nuclear force—under extreme conditions and to elucidate the fundamental properties of the strong interaction.

Collective flow phenomena observed in these collisions serve as crucial diagnostic tools for characterizing the QGP. When two heavy nuclei collide at relativistic speeds, a hot, dense, and short-lived medium with an anisotropic spatial profile is formed.[5–7] The collective motion of its constituents transforms this initial spatial anisotropy into a momentum-space anisotropy of the final-state particles. This anisotropic momentum distribution is quantitatively described by a Fourier decomposition of the azimuthal angle distribution, yielding flow harmonic coefficients (v_n). The second-order coefficient, elliptic flow (v_2), is dominant in mid-central collisions due to the initial elliptical overlap zone. Higher-order coefficients, like triangular flow (v_3), are also generated by event-by-event fluctuations in the initial nucleon positions. These coefficients are highly sensitive to the transport properties of the QGP, particularly the specific shear viscosity (η/s),[8,9] making them essential probes for extracting its fundamental properties.

Relativistic viscous hydrodynamic models have achieved remarkable success in describing the measured flow harmonics across a wide range of collision centralities, demonstrating excellent agreement with experimental data.[8–20] However, a persistent challenge, known as the v_3/v_2 puzzle, emerges when these models are applied to the most central, or "ultra-central", collisions (typically defined as the 0–1% or 0–2.5% of highest multiplicity events). Experimental measurements at the LHC, using two-particle cumulant methods, reveal that v_2 and v_3 are nearly equal in magnitude in these ultra-central collisions.[6,21,22] In contrast, conventional hydrodynamic models predict a significant hierarchy, with v_2 substantially larger than v_3.[23]

This puzzle has spurred extensive research efforts, primarily focused on four avenues: (1) refining the initial-state model to alter fluctuation profiles;[24–32] (2) investigating the nuanced effects of temperature-dependent transport coefficients;[33–36] (3) incorporating hydrodynamic fluctuations;[37–39] and (4) exploring different equations of state for the QGP.[40] While these studies have provided valuable insights, no single approach or combination thereof has yet fully resolved the puzzle within the standard hydrodynamic framework.

This suggests that a solution may require a more fundamental revision of the physical input, particularly concerning the initial state. In recent years, the study of nuclear structure has garnered significant attention in the

*Corresponding authors. Email: lgpang@ccnu.edu.cn; xnwang@ccnu.edu.cn

© 2026 Chinese Physical Society and IOP Publishing Ltd. All rights, including for text and data mining, AI training, and similar technologies, are reserved.

context of heavy-ion collisions. Notable advancements have been achieved in various areas, including deformed nuclei,[41–48] α clusters,[49–51] neutron halos,[52,53] and neutron skins.[54–57]

We hypothesize that the discrepancy lies in the model's handling of the initial state and its interplay with viscosity. Traditional models often employ a Woods–Saxon distribution to sample nucleon positions within the colliding nuclei. This approach generates substantial initial-state geometric eccentricities ϵ_n, particularly ϵ_2, due to large event-by-event fluctuations. To dampen this overly large initial ϵ_2 and reproduce the experimental v_2, the models require a relatively large specific shear viscosity. While this elevated viscosity successfully curbs ϵ_2, it suppresses the higher-order ϵ_3—and consequently the final v_3—even more severely. This results in a predicted v_3 that is too small compared to v_2, contradicting the near-equality observed in the data.[21]

The key to resolving the puzzle, therefore, lies not in further tuning the viscosity but in constructing a more physically realistic initial-state model that generates a smaller, more accurate initial ϵ_2 from the outset. A reduced initial eccentricity would permit the use of a smaller, more physically justified viscosity to match v_2, which would in turn apply less suppression to v_3, naturally bringing the model predictions into alignment with the $v_2 \approx v_3$ observation. Based on this insight, the present study introduces a novel approach to address the v_3/v_2 puzzle by implementing two crucial microphysical corrections to the initial state: (1) Nucleon Short-Range Repulsion: We enforce a minimum distance between nucleons during the sampling process to simulate the short-range repulsive core of the nucleon–nucleon interaction, which promotes a more uniform nucleon distribution and reduces initial-state fluctuations. (2) Sub-Nucleon Structure: We incorporate a model of proton internal structure ("hot spots") to provide a more granular and physically motivated description of the energy deposition, moving beyond the simple point-like nucleon approximation.

2. Methods.

2.1. Initial State Geometry. The atomic nucleus, comprising protons and neutrons, represents one of nature's most intricate quantum-mechanical systems. The spatial distribution of nucleons within the nucleus is commonly modeled using a Woods–Saxon distribution,

$$\rho(r) = \frac{\rho_0}{1 + \exp\left(\frac{r-R}{a}\right)}, \tag{1}$$

where, for a lead (Pb) nucleus, the parameters are $R = 6.62\,\mathrm{fm}$ and $a = 0.546\,\mathrm{fm}$, and ρ_0 is the saturated nuclear density.

To simulate the initial state geometry of nuclear collisions, several models have been developed. Among these, the Reduced Thickness Event-by-event Nuclear Topology (TRENTo) model[58,59] provides a computationally efficient and flexible parametric framework for generating initial conditions in high-energy nuclear collisions. Developed at Duke University, TRENTo incorporates event-by-event fluctuations in entropy density in the transverse plane, enabling it to describe higher-order anisotropic flow coefficients v_n. Owing to its versatility and success in fitting experimental data, TRENTo is adopted as the default initial-condition model in the public version of CLVisc.

The model is based on eikonal entropy deposition through a reduced-thickness function defined as

$$T_{\mathrm{R}}(T_{\mathrm{A}}, T_{\mathrm{B}}) = \left(\frac{T_{\mathrm{A}}^p + T_{\mathrm{B}}^p}{2}\right)^{1/p}, \tag{2}$$

where $T_{\mathrm{A,B}}(x,y) = \int \mathrm{d}z \rho_{\mathrm{A,B}}^{\mathrm{part}}(x,y,z)$ represents the participant thickness functions of the colliding nuclei. Physically, the parameter p interpolates among qualitatively distinct mechanisms for entropy production. Here, the parameter is set to $p = 0$, which is analogous to the initial condition in the IP-Glasma model. The TRENTo model has successfully described experimental proton–proton, proton–nucleus, and nucleus–nucleus multiplicity distributions, and it has generated nucleus–nucleus eccentricity harmonics consistent with experimental flow constraints. The root mean square eccentricities $\epsilon_n\{2\}$ can be expressed as

$$\epsilon_n\{2\} = \sqrt{\langle \epsilon_n \epsilon_n^* \rangle_{\mathrm{events}}}, \quad \epsilon_n = \left\langle r^n \mathrm{e}^{\mathrm{i}n\phi} \right\rangle, \tag{3}$$

with the complex eccentricity ϵ_n defined as

$$\epsilon_n = \frac{\int \mathrm{d}x\mathrm{d}y r^n \mathrm{e}^{\mathrm{i}n\phi} T_{\mathrm{R}}}{\int \mathrm{d}x\mathrm{d}y r^n T_{\mathrm{R}}}, \tag{4}$$

where T_{R} denotes the reduced thickness function from the TRENTo model, and the integrals are performed over the transverse plane.

In our study, we use the standard 2+1D TRENTo model to generate the transverse entropy density profile and extend it to 3D by introducing a separate parameterization for the longitudinal dependence. Specifically, we factorize the entropy density as

$$s(x,y,\eta_s) = s_{2\mathrm{D}}(x,y) H(\eta_s), \tag{5}$$

with the longitudinal profile given by

$$H(\eta_s) = \exp\left[-\frac{(|\eta_s| - \eta_{\mathrm{flat}})^2}{2\eta_{\mathrm{gw}}^2}\theta(|\eta_s| - \eta_{\mathrm{flat}})\right], \tag{6}$$

where $\eta_{\mathrm{flat}} = 2.0$ and $\eta_{\mathrm{gw}} = 1.8$ control the width and fall-off of the rapidity distribution.

2.2. The Uniformity of Nucleon Distribution within Nucleus. Inspired by Ref. [23], where nucleon–nucleon correlation plays a role in resolving the v_2 to v_3 ratio puzzle in ultra-central collisions, we hypothesize that this effect arises because the short-range repulsion introduced by nucleon–nucleon correlation leads to a more uniform distribution of nucleons within the nucleus. We pose the question: Could a uniformly distributed nucleon configuration within the nucleus fully resolve this puzzle? To address this, we manipulate the uniformity of nucleon distribution by varying the minimum distances between nucleons. Given that the single nucleon density and the charge radius of the nucleus are experimentally constrained, increasing

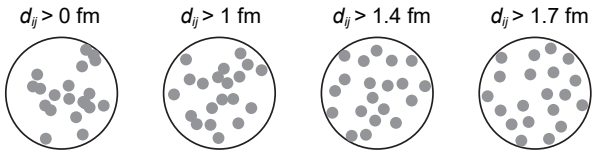

Fig. 1. A schematic diagram illustrating the homogenization effect arising from short-range nucleon–nucleon repulsions, achieved by modulating the minimum internucleon distance.

the minimum distance between nucleons enhances the uniformity of the nucleon distribution.

This is illustrated in Fig. 1, where 20 nucleons are sampled within a 2D circle of radius 5 fm. The same rejection method as in TRENTo is employed to discard newly sampled nucleons if their distance from previously sampled nucleons is less than the minimum distance d_{ij}. It is shown that with $d_{ij} = 0$ fm, the nucleons exhibit strong fluctuations and significant overlaps, which are unfavorable under the short-range repulsive potential. As d_{ij} increases from 0 fm to 1.7 fm, the nucleons are distributed more uniformly inside the nucleus. We aim to test the impact of this uniformity on the v_2 and v_3 ratios in ultra-central collisions.

Notably, as a proof-of-principle study, the minimum nucleon separation introduced here does not imply that nucleons cannot be closer in actual nuclei. Short-range correlations and the EMC effect have demonstrated the existence of nucleon pairs with high relative momenta and small spatial separations. As illustrated in Fig. 1, the minimum distance parameter offers a practical way to adjust the spatial homogeneity of nucleons within the nucleus. This modification corresponds to multi-nucleon correlations not captured by the Woods–Saxon distribution or short-range two-nucleon correlations. Furthermore, such multi-nucleon correlations in heavy nuclei remain challenging to extract from *ab initio* calculations.

2.3. Sub-Nucleon Structure. The sub-nucleon structure may affect the uniformity of the nucleon distribution. Specifically, proton structure has been experimentally observed to exhibit internal "hot spots", characterized by localized regions of high gluon density.[60] Within the framework of sub-nucleon studies, it is commonly assumed that a nucleon possesses N_c degrees of freedom. These degrees of freedom divide the nucleon into N_c Gaussian components. For the specific case of three constituent quarks, N_c is set to 3.[32,61,64,69] The transverse spatial coordinates of these constituent quarks within the nucleon are sampled from a normal distribution,

$$p(x,y) = \frac{1}{2\pi r^2}\exp\left[-\frac{(x-x')^2+(y-y')^2}{2r^2}\right], \quad (7)$$

where (x', y') denotes the transverse position of the parent nucleon, and r represents the constituent dispersion width, calculated as

$$r = \sqrt{\frac{w^2 - v^2}{1 - 1/N_c}}, \quad (8)$$

where w is the Gaussian width of a nucleon fixed to 0.5 fm, and v denotes the Gaussian width of a constituent quark, whose value is set to 0.3 fm.

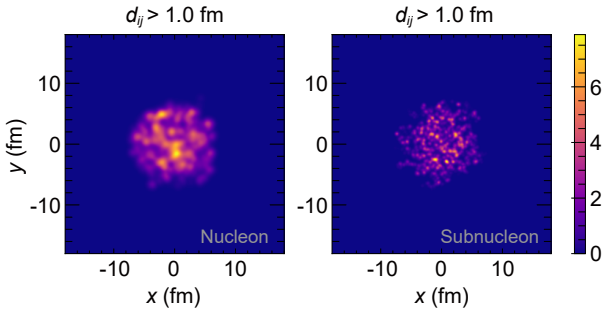

Fig. 2. The distribution of initial entropy density in the transverse plane for Pb+Pb collisions at $\sqrt{s_{\rm NN}} = 2.76$ TeV, with and without sub-nucleon fluctuations.

Figure 2 compares the initial entropy density distributions in the transverse plane for two ultra-central Pb+Pb collisions, with and without sub-nucleon fluctuations. The distributions exhibit significant visual differences. In the absence of sub-nucleon fluctuations, the entropy density distribution appears more diffuse. Conversely, when sub-nucleon fluctuations are included, the entropy density distribution becomes notably sharper. The size of each hot spot is considerably smaller in the presence of sub-nucleon fluctuations compared to the case without them. These observations suggest that the sub-nucleon structure influences the initial state fluctuations. However, it remains uncertain whether it also affects the uniformity of the distribution.

2.4. Hydrodynamics Simulation. We investigate the hydrodynamic response to these initial conditions using CLVisc,[14–20] a (3+1)-dimensional relativistic hydrodynamic model parallelized on graphics processing units (GPUs) using the Open Computing Language (OpenCL). This implementation achieves a 60-fold performance enhancement in spacetime evolution and over a 120-fold improvement in Cooper–Frye particlization compared to non-GPU parallelized computations. The model's validity is rigorously assessed through comparisons with various analytical solutions, existing numerical hydrodynamic approaches, and experimental data on hadron spectra from high-energy heavy-ion collisions.

The main equations of hydrodynamics are derived from the conservation laws of energy and momentum, expressed as

$$\nabla_\mu T^{\mu\nu} = 0, \quad (9)$$

where the energy-momentum tensor $T^{\mu\nu}$ is defined as $T^{\mu\nu} = \epsilon u^\mu u^\nu - P\Delta^{\mu\nu} + \pi^{\mu\nu}$. Here ϵ, P, u^μ, and $\pi^{\mu\nu}$ represent the energy density, pressure, four-velocity, and shear-stress tensor respectively. The projection operator is given by: $\Delta^{\mu\nu} = g^{\mu\nu} - u^\mu u^\nu$. The metric convention adapted throughout this work is $g^{\mu\nu} = \mathrm{diag}(1,-1,-1,-1)$ for Cartesian coordinates (t,x,y,z).

The dynamical models based on relativistic hydrodynamics have been successful in describing the anisotropic flow coefficients v_n. These quantities are also conveniently represented by the "flow vector" $V_n = v_n \exp(in\Phi_n)$ in each event. The V_n value reflects the hydrodynamic response of the produced medium to the nth order initial-state eccentricity vector,[12] denoted by $\boldsymbol{\epsilon}_n =$

$\epsilon_n \exp(in\psi_n)$. Model calculations show that V_n is approximately proportional to ϵ_n in general for $n = 2$ and 3, and for $n = 4$ in the case of central collisions.

We compute the root mean square of the flow harmonic coefficients V_n,

$$v_n\{2\} = \sqrt{\langle V_n V_n^* \rangle_{\text{events}}}, \quad V_n = \langle \exp(in\phi) \rangle \,, \tag{10}$$

where ϕ is the azimuthal transverse momentum angle, $\langle \cdots \rangle_{\text{events}}$ is the average for events,

$$\langle \cdots \rangle_{\text{events}} = \frac{\int \mathrm{d}^2 p_{\mathrm{T}} \dfrac{\mathrm{d}N}{2\pi p_{\mathrm{T}} \mathrm{d}p_{\mathrm{T}} \mathrm{d}\eta} (\cdots)}{\int \mathrm{d}^2 p_{\mathrm{T}} \dfrac{\mathrm{d}N}{2\pi p_{\mathrm{T}} \mathrm{d}p_{\mathrm{T}} \mathrm{d}\eta}}, \tag{11}$$

where the $\mathrm{d}N/(2\pi p_{\mathrm{T}} \mathrm{d}p_{\mathrm{T}} \mathrm{d}\eta)$ represents particle distributions in the transverse momentum range at the central rapidity region.

In our computational framework, the lattice dimensions are configured as $n_x \times n_y \times n_z = 300 \times 300 \times 161$. The hydrodynamic evolution is solved on a three-dimensional lattice covering $|x|, |y| < 18\,\text{fm}$ and $|\eta_s| < 9.6$, with uniform lattice spacings $\Delta_x = \Delta_y = \Delta_{\eta_s} = 0.12$, and a thermalization time of $\tau_0 = 0.6\,\text{fm}$. The equation of state utilized in our simulations is the one from "s95-v1-PCE165".[65] Additionally, we adopted a freeze-out temperature of $T = 0.137\,\text{GeV}$. For each configuration of the model parameters, we generated 1000 hydrodynamic events.

3. Results. In this section, we first calibrate our model using pseudo-rapidity distributions, transverse momentum spectra, and flow coefficients of charged hadrons in Pb+Pb collisions at $\sqrt{s_{\text{NN}}} = 2.76\,\text{TeV}$. Then we investigate the effect of nuclear and sub-nucleon structure on the initial eccentricity at the 0–1% centrality for different minimum distances using the TRENTo model. Finally, we present numerical results for flow harmonics across a range of minimum distances and centralities, obtained with the TRENTo initial conditions and the CLVisc hydrodynamic model.

3.1. Code Calibration. Figure 3 (from upper to lower) presents the pseudo-rapidity distributions of charged hadrons in four distinct centrality classes, 0–5%, 5%–10%, 10%–20%, and 20%–30%, obtained from CLVisc simulations, compared with experimental data from the ALICE collaboration. The simulation results, with a minimum distance between nucleon pairs $d_{\text{min}} = 1.4\,\text{fm}$, exhibit good agreement with the experimental data. This comparison serves to calibrate model parameters in relativistic hydrodynamic simulations for the most central collisions. Initially, we hypothesized that varying d_{min} might alter the centrality dependence, thereby undermining the predictive power of relativistic hydrodynamics for other centrality ranges when parameters are fixed using the 0–5% centrality range, as observed in O-O collisions considering α clusters.[49] Contrary to our hypothesis, d_{min} does not influence the centrality dependence. This outcome may be attributed to the fact that α clusters induce more substantial changes to the nuclear structure of ^{16}O than the modifications we applied to ^{208}Pb.

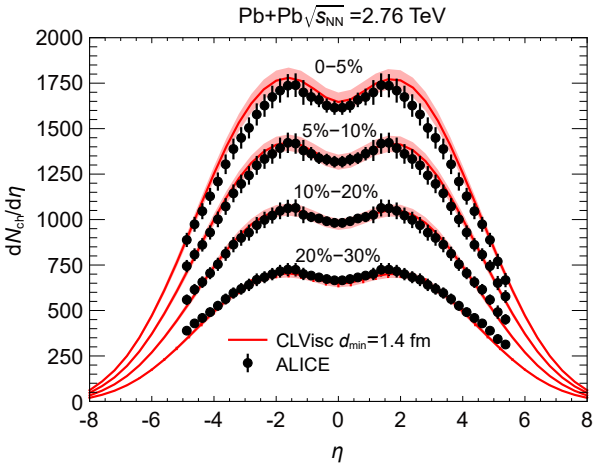

Fig. 3. Pseudorapidity distribution for charged hadron in Pb+Pb collisions at $\sqrt{s_{\text{NN}}}$ =2.76 TeV with centrality range 0–5%, 5%–10%, 10%–20%, and 20%–30%, from CLVisc (the shear viscosity $\eta/s = 0.16$) and LHC experimental data by the ALICE collaboration.[66]

Figure 4 presents a comparative analysis of high-order differential flow between CLVisc simulations and ALICE experimental data across four centrality ranges 0–5%, 5%–10%, 10%–20%, and 20%–30%. The figure sequentially displays differential flow coefficients v_2, v_3, v_4 from top to bottom at low p_{T}. The simulations employed a Woods–Saxon distribution with a minimum distance parameter of 1.4 fm. The results show good agreement between the model and experimental data for v_2 and v_4. These findings suggest that relativistic hydrodynamic simulations provide a satisfactory description of p_{T}-differential v_n in semi-central collisions. However, the ultra-central puzzle remains and requires examination using p_{T} integrated v_n. In semi-central collisions, an excess in the high-p_{T} region of the p_{T} spectra may lead to slight discrepancies in p_{T}-integrated v_n, especially for the 0–5% centrality. Notably, for 0–5% centrality, v_3 exceeds v_2 at $p_{\mathrm{T}} > 2\,\text{GeV}$.

Figure 5 shows the transverse momentum spectra of charged hadrons as compared with experimental data, for four distinct centrality classes, 0–5%, 5%–10%, 10%–20%, and 20%–30%. The red lines correspond to CLVisc simulations with $\eta/s = 0.16$ and the black dots represent experimental data from the ALICE collaboration. Our observations indicate that a larger shear viscosity coefficient (η/s) suppresses the high-momentum hadron spectrum, making it more consistent with the experimental data. However, hydrodynamic simulations tend to overestimate the high transverse momentum charged hadron spectra compared to the experimental data from the ALICE Collaboration, while trying to describe the anisotropic flows. This suggests that incorporating bulk viscosity into the 3+1-dimensional viscous hydrodynamics framework may be necessary to improve the accuracy of the simulations.

3.2. Initial Eccentricities. The initial eccentricity exhibits an approximate linear relationship with the final collective flow that $v_n = k\epsilon_n$. Therefore, we first analyze the

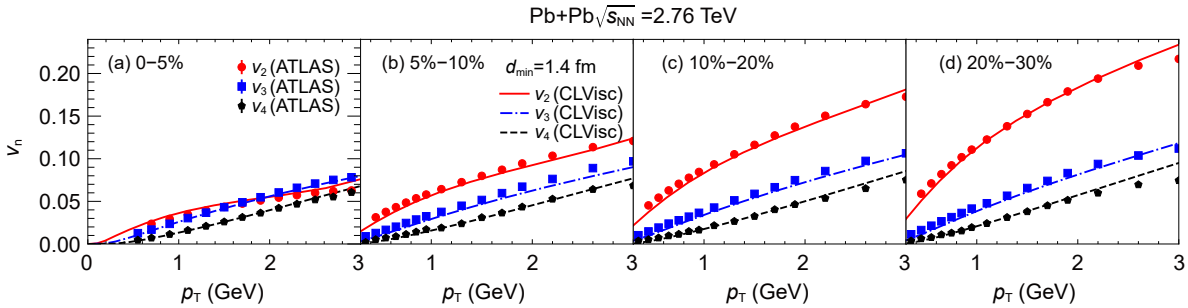

Fig. 4. Comparison of anisotropic flow coefficients v_2, v_3, and v_4 obtained via the event plane method in Pb+Pb collisions at $\sqrt{s_{NN}} = 2.76$ TeV for centrality classes 0–5%, 5%–10%, 10%–20%, and 20%–30%. Results from CLVisc hydrodynamic simulations (solid curves) with shear viscosity $\eta/s = 0.16$ are compared with experimental data (points) from the ATLAS Collaboration.[68]

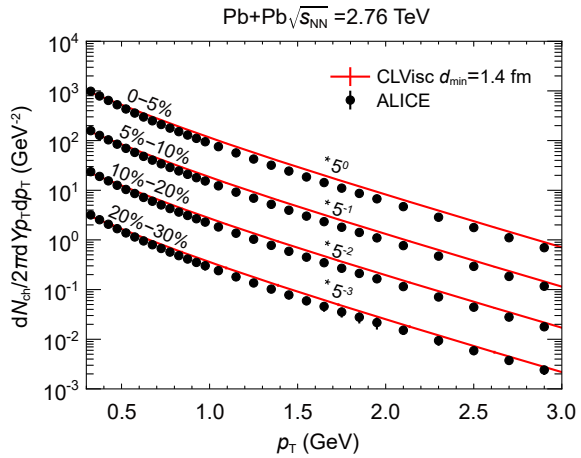

Fig. 5. The transverse momentum spectra of charged hadron in Pb+Pb collision at $\sqrt{s_{NN}} = 2.76$ TeV. Comparison of CLVisc hydrodynamic model calculations (curves) with the shear viscosity $\eta/s = 0.16$ with ALICE experimental measurements (points)[67] for four centrality classes: 0–5%, 5%–10%, 10%–20%, and 20%–30%.

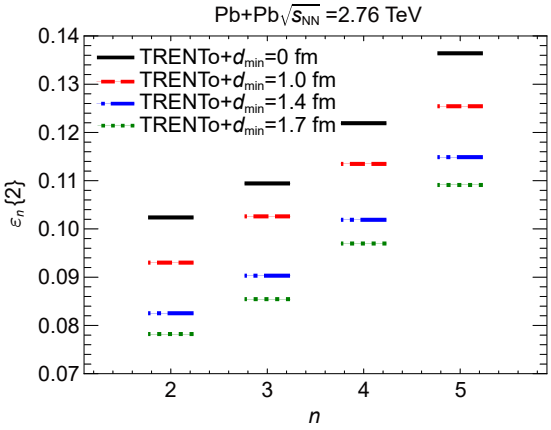

Fig. 6. The root mean square of eccentricities $\epsilon_n\{2\}$ calculated using the TRENTo initial condition model for 0–1% centrality Pb+Pb collisions. The black line is minimum distance of nucleon-nucleon $d_{min} = 0.0$ fm (solid line), $d_{min} = 1.0$ fm (red dashed line), $d_{min} = 1.4$ fm (blue dash-dot line), and $d_{min} = 1.7$ fm (green dotted line).

influence of the minimum distance on the initial eccentricity. The centrality of the collisions was determined using the total entropy of each event from the TRENTo model. For example, to select events within the 0–5% centrality range, all events were sorted based on the total entropy in descending order, and the top 5% of events were selected. This does not change the overall order of events sorted by charged multiplicity. Experimentally, the most central 0–0.2% centrality is determined using both multiplicity at midrapidity ($|\eta| < 2.5$) and transverse energy E_T sum at forward rapidity ($2.9 < |\eta| < 5.2$).[21] Events are selected based on two criteria: a summed transverse energy (E_T) exceeding 3260 GeV and a charged-particle multiplicity greater than 9500 (over 5 units of pseudorapidity). The intersection of these events constitutes 0.2% of the total, defining the 0–0.2% centrality class. For other centrality classes, the definition relies exclusively on the summed E_T at forward rapidity. As a cross-check, the 0–1% centrality range is also examined using both multiplicity and transverse energy sum, analogous to the selection for the 0–0.2% ultra-central events. The flow harmonics v_n derived from these two centrality determination methods are consistent within statistical uncertainties. In our model, both centrality determination methods yield identical centrality classes. In principle, a more realistic model incorporating forward rapidity fluctuations would be required to accurately align with the experimental centrality definition. This limitation of our current hydrodynamic framework will be addressed in future work.

Figure 6 illustrates the root mean square eccentricities $\epsilon_n\{2\}$, for $n = 2$–6, in Pb-Pb collisions within the 0–1% centrality class, as a function of the minimum distance between nucleons. The data reveal that as the minimum distance increases, the root mean square eccentricities exhibit a gradual decrease, with the rate of decrease remaining approximately constant. Notably, higher-order eccentricities are significantly larger than the second-order eccentricities. The results are presented for the TRENTo model, which indicates that an increase in the minimum distance between nucleons correlates with a reduction in fluctuations in the initial conditions, where the eccentricity primarily arises from fluctuations in the initial nucleon states.

Figure 7 illustrates the effect of sub-nucleon fluctuations. It is shown that these fluctuations lead to a reduction in the initial eccentricity, with a stronger suppression observed for the second-order eccentricity compared to the third-order. This differential suppression is expected to

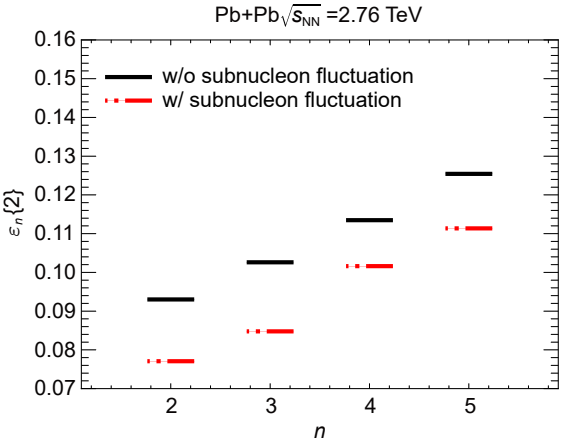

Fig. 7. The root mean square of eccentricities $\epsilon_n\{2\}$ in 0–1% central Pb+Pb collisions calculated using the TRENTo initial condition model. The black solid line ($d_{\min} = 1.0$ fm) and red dashed line ($d_{\min} = 1.0$ fm and sub-nucleon fluctuations) represent the model predictions.

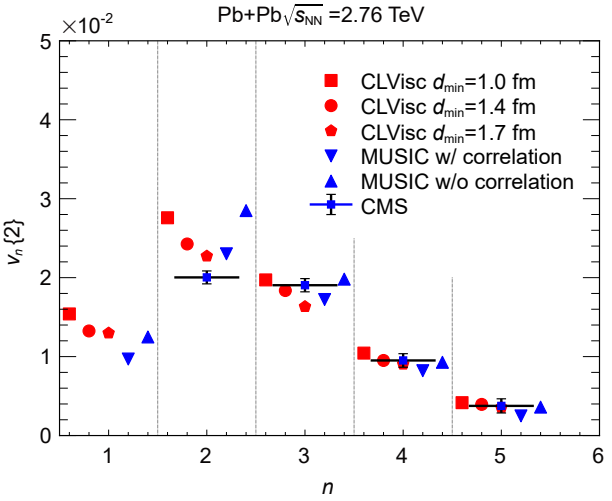

Fig. 8. The flow harmonics, $v_n\{2\}$, for the TRENTo initial conditions and CLVisc hydrodynamics models are presented. The red square corresponds to the minimum distance ($d_{\min} = 1.0$ fm), the red circle ($d_{\min} = 1.4$ fm), and the red pentagon ($d_{\min} = 1.7$ fm). Additionally, the blue upper triangle represents the scenario without nucleon–nucleon correlations, while the blue down triangle corresponds to the case with nucleon–nucleon correlations, both derived from the IP-glasma+MUSIC model. [23]

improve the v_3/v_2 ratio.

3.3. Flow Harmonic Coefficients. Figure 8 presents the flow harmonic coefficients $v_n\{2\}$ for minimum distances $d_{\min} = 1.0$, 1.4, and 1.7 fm, considering both the nucleon–nucleon correlation (MUSIC+IP-glasma) and without nucleon–nucleon correlation, for ($n = 2$–5), in Pb-Pb collisions at $\sqrt{s_{\rm NN}} = 2.76$ TeV within the 0–1% centrality class, for charged hadrons. Notably, compared to the 0–5% centrality class, the more central 0–1% centrality class in Pb-Pb collisions appears to require a higher shear viscosity to entropy density ratio η/s. Consequently, a value of $\eta/s = 0.22$ was employed in this analysis. To facilitate comparison with experimental data, a cut-off of 0.3–3 GeV was applied to the transverse momentum integrals. We find that the result of the minimum distance $d_{\min} = 1.4$ fm improves the previous results, leading to a better agreement with the CMS data. [21]

Figure 9 shows comparison between hydrodynamic simulation results with centrality of 0–0.2%, 0–1%, 0–2.5%, 2.5%–5% and experimental data from CMS. [21] And we find that the results from fluid dynamics are nearly consistent with experimental results for centrality ranges of 2.5%–5%. However, for other centralities, the minimization of the distance improved the consistency between the hydrodynamics results and experimental values of $v_2\{2\}$ and $v_3\{2\}$. For other higher-order flows, the hydrodynamic simulation aligns well with the experimental observations.

Figure 10 illustrates the influence of sub-nucleon fluctuations on flow coefficients in ultra-central collisions. A comparison of experimental data with calculations from two different initial condition models, including scenarios with and without sub-nucleon fluctuations $d_{\min} = 1.0$ fm, provides a clear evaluation of the impact of sub-nucleon fluctuations on the hydrodynamic final state. For Pb+Pb collisions at $\sqrt{s_{\rm NN}} = 2.76$ TeV within the 0–1% centrality range, the predictions for the second-order flow coefficient $v_2\{2\}$ and the ratio of $v_3\{2\}$ to $v_2\{2\}$ demonstrate that results incorporating sub-nucleon fluctuations align more closely with experimental observations than those without.

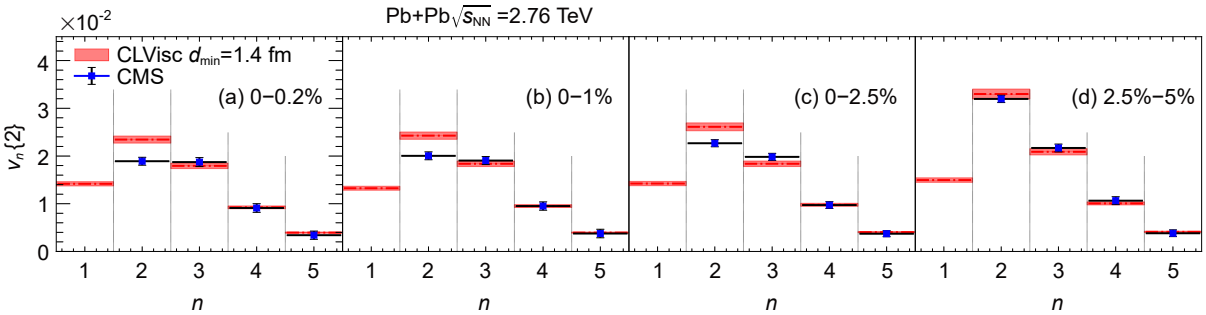

Fig. 9. The flow harmonics, $v_n\{2\}$, calculated using TRENTo initial conditions coupled to CLVisc hydrodynamic simulations with shear viscosity $\eta/s = 0.22$, compared with CMS experimental data. Results are shown for four centrality classes: 0–0.2%, 0–1%, 0–2.5%, and 2.5%–5%. The red line displays model predictions using a minimum nucleon–nucleon distance $d_{\min} = 1.4$ fm, while black line represent CMS experimental measurements. Vertical error bars indicate statistical uncertainties in experimental data, with shaded color bands corresponding to theoretical statistical uncertainties from the model calculations.

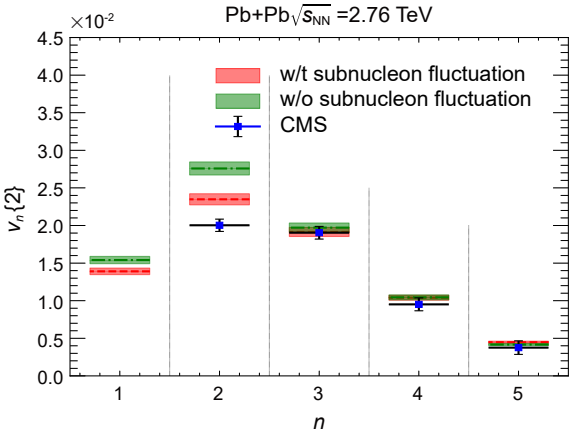

Fig. 10. Comparison of the flow coefficient $v_n\{2\}$ between experimental data and theoretical predictions from two scenarios: (1) $d_{\min} = 1.0\,\text{fm}$ ($\eta/s = 0.22$) and (2) sub-nucleon fluctuations with $d_{\min} = 1.0\,\text{fm}$ ($\eta/s = 0.18$), for Pb+Pb collisions at $\sqrt{s_{\text{NN}}} = 2.76\,\text{TeV}$ within the 0–1% centrality range, as calculated by CLVisc. The experimental uncertainties are indicated by error bars, while the theoretical statistical uncertainties are represented by shaded color bands.

4. Discussion and Summary. The $v_2\{2\}$ to $v_3\{2\}$ ratio puzzle in ultra-central heavy ion collisions remains an unresolved challenge. Previous studies have shown that modifying the two-nucleon distribution within the colliding nucleus can bring the $v_2\{2\}$ to $v_3\{2\}$ ratio closer to experimental data, but this modification has not fully resolved the puzzle. We hypothesize that this discrepancy may be due to more intricate nuclear structure effects within the nucleus, which render the nucleon distribution within the nucleus inadequately represented by a simple Woods–Saxon distribution. To explore this possibility, we conducted a preliminary investigation by altering the minimum distance between nucleons within the nucleus and incorporating sub-nucleon fluctuations within nucleons to modify the nuclear structure and observe its impact on the $v_2\{2\}$ to $v_3\{2\}$ ratio.

Our findings indicate that increasing the minimum distance between nucleons reduces the geometric eccentricity of all orders. Consequently, this reduction allows for a smaller shear viscosity to entropy density ratio (η/s) in relativistic hydrodynamic simulations to achieve a $v_2\{2\}$ to $v_3\{2\}$ ratio that aligns more closely with experimental data. Without increasing the minimum nucleon distance, the higher geometric eccentricities necessitate a larger η/s to match the experimental $v_2\{2\}$, which in turn leads to a stronger suppression of higher-order anisotropic flows.

Our study suggests that nuclear structure indeed plays a role in resolving the $v_2\{2\}$ to $v_3\{2\}$ ratio puzzle in ultra-central heavy ion collisions. However, this resolution is intertwined with other effects, such as the reduction in the required shear viscosity, which mitigates the damping effect of viscosity on higher-order anisotropies. It is important to note that our current research focuses on one aspect of the puzzle and does not comprehensively consider other factors that may influence it, such as bulk viscosity [70,71] and hydrodynamic fluctuations. A thorough resolution of the puzzle will require future studies that integrate all relevant effects.

Additionally, our findings indicate that sub-nucleon fluctuations also play a significant role in addressing the $v_2\{2\}$ to $v_3\{2\}$ ratio puzzle in ultra-central heavy ion collisions. This phenomenon can be attributed to the enhanced spatial homogeneity of the QGP initial geometry. Considering sub-nucleon effects, the initial eccentricity decreases, with the second-order eccentricity decreasing more than the third-order eccentricity, which offers substantial explanatory power for resolving this longstanding puzzle in collective flow phenomenology.

The minimum-distance constraint serves as an effective phenomenological proxy for multi-nucleon correlations, particularly the repulsive core in nuclear interactions, which collectively dilute the nuclear density and moderate initial-state fluctuations. Similarly, sub-nucleon degrees of freedom contribute to a smoother initial geometry, reinforcing the differential suppression of anisotropic flow coefficients.

The influence of pileup events on the $v_2\{2\}$ to $v_3\{2\}$ ratio puzzle in ultra-central events is proved to be negligible. [21] Pileup events, which occur when two collisions are recorded within a single beam crossing, are typically identified by experimentalists through the correlation of energy sum signals between the Zero Degree Calorimeter (ZDC) and Hadron Forward (HF) detectors. Events with large signals are labeled as pileup events, which constitute approximately 0.1% of all events. These events are subsequently rejected, and the results remain stable within less than 1% when varying the ZDC sum energy requirements for pileup rejection, as demonstrated in the CMS experiment. [21]

One limitation of this study is the absence of bulk viscosity. It has been demonstrated that bulk viscosity reduces the mean transverse momentum, thereby decreasing both the integrated v_2 and v_3. Lowering η/s can help reproduce the same v_2. However, after this adjustment, the v_3/v_2 ratio remains unaffected by bulk viscosity, and the puzzle persists. [71]

Furthermore, our findings underscore the sensitivity of ultra-central heavy-ion collision events to nuclear structure. The unresolved puzzles in heavy-ion collisions may necessitate interdisciplinary research that bridges high-energy nuclear physics with low-energy nuclear physics to jointly address these challenges and drive progress in both fields. In conclusion, while our study provides insights into the $v_2\{2\}$ to $v_3\{2\}$ ratio puzzle, a comprehensive understanding remains an ongoing endeavor that will benefit from a synergistic approach across different areas of nuclear physics. Our approach substantially improves the description of ultra-central flow observables and helps to address the ultra-central flow puzzle.

Meanwhile, a parallel study was recently reported on arXiv, wherein the authors addressed the v_2/v_3 puzzle by incorporating a "breathing" octupole mode in the ^{208}Pb nucleus. [48] Although their approach differs from ours, both studies emphasize the key role of nuclear structure

in resolving this issue, underscoring the importance of this research direction.

Acknowledgements. This work was supported by the National Natural Science Foundation of China (Grant Nos. 12075098, 12535010, 12435009, and 1193507) and the Guang-dong MPBAR (Grant No. 2020B0301030008). The numerical calculation have been performed on the GPU cluster in the Nuclear Science Computing Center at Central China Normal University (NSC3).

References

[1] Gyulassy M and McLerran L 2005 *Nucl. Phys. A* **750** 30
[2] Jamil M and Rhee J T 2009 *Contemp. Phys.* **50** 665
[3] Yagi K, Hatsuda T and Miake Y 2005 *Quark-Gluon Plasma: From Big Bang to Little Bang* (Cambridge University Press)
[4] Ellis J 2006 *J. Phys. Conf. Ser.* **50** 8
[5] Aamodt K, Abelev B, Abrahantes Quintana A *et al.* (ALICE Collaboration) 2010 *Phys. Rev. Lett.* **105** 252302
[6] Aamodt K, Abelev B, Abrahantes Quintana A *et al.* (ALICE Collaboration) 2011 *Phys. Rev. Lett.* **107** 032301
[7] Abelev B, Adam J, Adamová D *et al.* (ALICE Collaboration) 2015 *JHEP* **06** 190
[8] Heinz U, Song H, and Chaudhuri A K 2006 *Phys. Rev. C* **73** 034904
[9] Song H and Heinz U 2008 *Phys. Rev. C* **77** 064901
[10] Song H, Bass S A, Heinz U, Hirano T, and Shen C 2011 *Phys. Rev. Lett.* **106** 192301
[11] Shen C, Qiu Z, Song H C, Bernhard J, Bass S, and Heinz U 2016 *Comput. Phys. Commun.* **199** 61
[12] Gardim F G, Grassi F, Luzum M, and Ollitrault J Y 2012 *Phys. Rev. C* **85** 024908
[13] Ding C, Ke W Y, Pang L G, and Wang X N 2021 *Chin. Phys. C* **45** 074102
[14] Pang L G, Petersen H, and Wang X N 2018 *Phys. Rev. C* **97** 064918
[15] Pang L G, Petersen H, Qin G Y, Roy V, and Wang X N 2016 *Nucl. Phys. A* **956** 272
[16] Pang L G, Petersen H, Qin G Y, Roy V, and Wang X N 2016 *Eur. Phys. J. A* **52** 97
[17] Pang L G, Qin G Y, Roy V, Wang X N, and Ma G L 2015 *Phys. Rev. C* **91** 044904
[18] Schenke B, Jeon S, and Gale C 2010 *Phys. Rev. C* **82** 014903
[19] Shen C, Paquet J F, Denicol G S, Jeon S, and Gale C 2017 *Phys. Rev. C* **95** 014906
[20] Wu X Y, Qin G Y, Pang L G, and Wang X N 2022 *Phys. Rev. C* **105** 034909
[21] Chatrchyan S, Khachatryan V, Sirunyan A M *et al.* (CMS Collaboration) 2014 *JHEP* **02** 088
[22] Aad G, Abbott B, Abdallah J *et al.* (ATLAS Collaboration) 2012 *Phys. Rev. C* **86** 014907
[23] Denicol G S, Gale C, Jeon S, Paquet J F, and Schenke B 2014 arXiv:1406.7792 [nucl-th]
[24] Petersen H, Qin G Y, Bass S A, and Müller B 2010 *Phys. Rev. C* **82** 041901
[25] Giacalone G, Guerrero-Rodríguez P, Luzum M, Marquet C, and Ollitrault J Y 2019 *Phys. Rev. C* **100** 024905
[26] Snyder R, Byres M, Lim S H, and Nagle J L 2021 *Phys. Rev. C* **103** 024906
[27] Bhalerao R S, Giacalone G, Guerrero-Rodríguez P, Luzum M, Marquet C, and Ollitrault J Y 2019 *Acta Phys. Pol. B* **50** 1165
[28] Shen C, Qiu Z, and Heinz U 2015 *Phys. Rev. C* **92** 014901
[29] Carzon P, Rao S, Luzum M, Sievert M, and Noronha-Hostler J 2020 *Phys. Rev. C* **102** 054905
[30] Zakharov B G 2020 *JETP Lett.* **112** 393
[31] Santos L 2024 *Braz. J. Phys.* **54** 232
[32] Loizides C 2016 *Phys. Rev. C* **94** 024914
[33] Lacey R A 2024 *Phys. Rev. C* **110** L031901
[34] Luzum M and Ollitrault J Y 2013 *Nucl. Phys. A* **904-905** 377
[35] Rose J B, Paquet J F, Denicol G S, Luzum M, Schenke B, Jeon S Y, and Gale G 2014 *Nucl. Phys. A* **931** 926
[36] Giannini A V, Ferreira M N, Hippert M *et al.* (ExTrEMe Collaboration) 2023 *Phys. Rev. C* **107** 044907
[37] Kuroki K, Sakai A, Murase K, and Hirano T 2023 *Phys. Lett. B* **842** 137958
[38] Rybczynski M and Broniowski W 2016 *Acta Phys. Pol. B* **47** 1033
[39] Adam J, Adamová D, Aggarwal M M *et al.* (ALICE Collaboration) 2016 *Phys. Rev. Lett.* **117** 182301
[40] Alba P, Mantovani Sarti V, Noronha J, Noronha-Hostler J, Parotto P, Portillo Vazquez I, and Ratti C 2018 *Phys. Rev. C* **98** 034909
[41] Abdulhamid M I, Aboona B E, Adam J *et al.* (STAR Collaboration) 2024 *Nature* **635** 67
[42] Giacalone G 2020 *Phys. Rev. Lett.* **124** 202301
[43] Giacalone G, Jia J, and Zhang C 2021 *Phys. Rev. Lett.* **127** 242301
[44] Dimri A, Bhatta S, and Jia J 2023 *Eur. Phys. J. A* **59** 45
[45] Wang Z, Chen J, Xu H, and Zhao J 2024 *Phys. Rev. C* **110** 034907
[46] Zhao S, Xu H, Zhou Y, Liu Y X, and Song H 2024 *Phys. Rev. Lett.* **133** 192301
[47] Xu H J, Zhao J, and Wang F 2024 *Phys. Rev. Lett.* **132** 262301
[48] Xu H J, Xu D, Zhao S, Zhao W, Song H, and Wang F 2025 arXiv:2504.19644 [nucl-th]
[49] Ding C, Pang L G, Zhang S, and Ma Y G 2023 *Chin. Phys. C* **47** 024105
[50] Wang Y, Zhao S, Cao B, Xu H, and Song H 2024 *Phys. Rev. C* **109** L051904
[51] Bijker R and Iachello F 2017 *Nucl. Phys. A* **957** 154
[52] Zhou S G, Meng J, Ring P, and Zhao E G 2010 *Phys. Rev. C* **82** 011301
[53] Habs D, Gross M, Thirolf P G, and Böni P 2011 *Appl. Phys. B* **103** 485
[54] Liu Q, Zhao S, Xu H J, and Song H 2024 *Phys. Rev. C* **109** 034912
[55] Li H, Xu H J, Zhou Y, Wang X, Zhao J, Chen L W, and Wang F 2020 *Phys. Rev. Lett.* **125** 222301
[56] Adhikari D, Albataineh H, Androic D *et al.* (PREX Collaboration) 2021 *Phys. Rev. Lett.* **126** 172502
[57] Giacalone G, Nijs G, and van der Schee W 2023 *Phys. Rev. Lett.* **131** 202302
[58] Moreland J S, Bernhard J E, and Bass S A 2015 *Phys. Rev. C* **92** 011901
[59] Ke W, Moreland J S, Bernhard J E, and Bass S A 2017 *Phys. Rev. C* **96** 044912
[60] De Roeck A 1992 *Nucl. Phys. B Proc. Suppl.* **29** 61
[61] Bernhard J E, Scott Moreland J, Bass S A *et al.* 2016 *Phys. Rev. C* **94** 024907
[62] Mäntysaari H and Schenke B 2017 *Phys. Lett. B* **772** 832
[63] Mäntysaari H, Salazar F, Schenke B, Shen C, and Zhao W 2024 *EPJ Web Conf.* **296** 10001
[64] Zhu J, Wu X Y, and Qin G Y 2025 *Chin. Phys. C* **49** 044103
[65] Huovinen P and Petreczky P 2010 *Nucl. Phys. A* **837** 26
[66] Adam J, Adamová D, Aggarwal M M *et al.* (ALICE Collaboration) 2017 *Phys. Lett. B* **772** 567.
[67] Abelev B, Adam J, Adamová D *et al.* (ALICE Collaboration) 2013 *Phys. Lett. B* **720** 52
[68] Aad G, Abbott B, Abdallah J *et al.* (ATLAS Collaboration) 2012 *Phys. Rev. C* **86** 014907
[69] Nijs G, van der Schee W, Gürsoy U, and Snellings R 2021 *Phys. Rev. C* **103** 054909
[70] Everett D, Ke W, Paquet J F *et al.* (JETSCAPE Collaboration) 2021 *Phys. Rev. C* **103** 054904
[71] Rose J B, Paquet J F, Denicol G S *et al.* 2014 *Nucl. Phys. A* **931** 926